frontiers in Materials

ORIGINAL RESEARCH
published: 16 November 2021
doi: 10.3389/fmats.2021.764455

Strong Electrorheological Performance of Smart Fluids Based on TiO_2 Particles at Relatively Low Electric Field

Yuchuan Cheng[1,2], Zihui Zhao[1,2,3], Hui Wang[1], Letian Hua[1], Aihua Sun[1], Jun Wang[3], Zhixiang Li[1], Jianjun Guo[1]* and Gaojie Xu[1]*

[1]Zhejiang Key Laboratory of Additive Manufacturing Materials, Ningbo Institute of Materials Technology and Engineering, Chinese Academy of Sciences, Ningbo, China, [2]Center of Materials Science and Optoelectronics Engineering, University of Chinese Academy of Sciences, Beijing, China, [3]Fujian Key Laboratory of Functional Marine Sensing Materials, Center for Advanced Marine Materials and Smart Sensors, Minjiang University, Fuzhou, China

Electrorheological (ER) fluids are a type of smart material with adjustable rheological properties. Generally, the high yield stress (>100 kPa) requires high electric field strength (>4 kV/mm). Herein, the TiO_2 nanoparticles were synthesized via the sol–gel method. Interestingly, the ER fluid-based TiO_2 nanoparticles give superior high yield stress of 144.0 kPa at only 2.5 kV/mm. By exploring the characteristic structure and dielectric property of TiO_2 nanoparticles and ER fluid, the surface polar molecules on samples were assumed to play a crucial role for their giant electrorheological effect, while interfacial polarization was assumed to be dominated and induces large yield stress at the low electric field, which gives the advantage in low power consumption, sufficient shear stress, low leaking current, and security.

Keywords: electrorheology, TiO_2, yield stress, dielectric property, complex fluid

OPEN ACCESS

Edited by:
Bo Li,
Xi'an Jiaotong University, China

Reviewed by:
Xufeng Dong,
Dalian University of Technology, China
Rongjia Tao,
Temple University, United States

****Correspondence:***
Yuchuan Cheng
yccheng@nimte.ac.cn
Jianjun Guo
jjguo@nimte.ac.cn

Specialty section:
This article was submitted to Smart Materials, a section of the journal Frontiers in Materials

Received: *25 August 2021*
Accepted: *05 October 2021*
Published: *16 November 2021*

Citation:
Cheng Y, Zhao Z, Wang H, Hua L, Sun A, Wang J, Li Z, Guo J and Xu G (2021) Strong Electrorheological Performance of Smart Fluids Based on TiO_2 Particles at Relatively Low Electric Field. Front. Mater. 8:764455. doi: 10.3389/fmats.2021.764455

1 INTRODUCTION

Electrorheological (ER) fluids are a kind of smart ER fluids, which are composed of polarizable solid particles and non-polar liquid medium. When an external DC electric field is applied, the rheological properties of ER fluids display continuous, rapid, and reversible changes (Halsey, 1992; Wen et al., 2008; Hwang et al., 2016; Su et al., 2016; Tao et al., 2016; Kim et al., 2017). This characteristic makes ER fluids have broad application prospects in the fast-acting valves, clutches, brakes, shock absorbers, inaccurate polishings, and robotics (Gamota and Filisko, 1991; Zhao et al., 2003; Wen et al., 2004). This has made ER fluids a persistent area of study in soft matter research, ever since their discovery several decades ago. Special interest has been given to TiO_2 as a promising candidate for high-performance ER materials, owing to its high permittivity (ε_{rutile} = 90~100, $\varepsilon_{anatase}$ = 30~40) (Yin and Zhao, 2004a; Ji et al., 2017). However, the ER performance of the crystalline TiO_2-based ER fluids is very bad, with only several kPa generally (e.g., 0.6 kPa at 4 kV/mm, Yin and Zhao, 2004a). The phenomenon is not consistent with conventional polarization mechanisms. In previous studies, many researchers have done effective ways to enhance the performance of TiO_2 ER fluids (Whittle and Bullough, 1992; He et al., 2017). Yin and Zhao (2004a) noticed that the crystalline TiO_2, dominated by fast ionic or atomic polarization, could not supply high ER activity with optimal dielectric or polarization properties. Furthermore, several strategies, including new synthesis method (microwave-assisted) (Plachy et al., 2015), surface coating/modification by polar molecules (Shen

et al., 2005; Wang et al., 2007a; Cheng et al., 2008; Niu et al., 2014), 2D nanosheets (He et al., 2018), internal structure activation by metal ions (Zhao and Yin, 2002a; Zhao and Yin, 2002b; Wang and Zhao, 2003; Yin and Zhao, 2004b), and doping with chromium (Cr) (Almajdalawi et al., 2013), have been developed to increase the ER response. However, despite the broad interest, applications have been hampered by the weakness of the ER effect (still generally less than 5 kPa, too low to meet the requirements for practical applications).

In recent years, a new group of giant ER fluids, consisting of amorphous TiO_2 and $MTiO(C_2O_4)_2$ (M=Ca, Ba, Sr) nanoparticles, which are coated with deliberately chosen polar molecules, showing high yield stress up to over 200 kPa under an applied electric field of 5 kV/mm, was developed (Wen et al., 2003; Shen et al., 2005; Huang et al., 2006; Wang et al., 2007a; Wang et al., 2007b; Cheng et al., 2008). The induced polarization model of dielectric ER fluids cannot explain many phenomena of these ER fluids. An obvious character of these ER fluids is not the quadratic dependence of yield stress but the linear dependence upon the electric field for the dielectric ER fluids.

So far, much theoretical analysis has also been adopted to explain the high yield stress of giant ER fluids, and the interaction between induced charges and polar molecules adsorbed on particle surfaces is generally assumed to be a key for Ca-Ti-O in understanding the giant ER effect (Shen et al., 2005; Wang et al., 2007a). However, up to now, high-performance ER fluids with strong yield stress (>100 kPa) still suffer from high electric field (up to 5 kV/mm) (Wang et al., 2007a). The irreproducibility of ER fluids, low colloidal stability, insufficient shear stress, or wear of pipes and valves still limit their industrial applications (Wang et al., 2005; Lu et al., 2007; Shen et al., 2009).

Herein, we present a new TiO_2 ER fluid with a strong ER response (106.8 kPa) at a low electric field (1.5 kV/mm). This yield stress in such a lower electric field is several orders higher than the reported giant ER fluids. The novel characteristic of the high yield stress at the low electric field may have many advantages, such as low power consumption, sufficient shear stress, low leaking current, and security.

2 EXPERIMENTAL SECTION

2.1 Materials

Tetrabutyl titanate (TBT, >98%) was bought from Aladdin Biochemical Technology Co., Ltd. (Shanghai, China). Absolute ethanol (C_2H_5OH, AR), acetic acid (CH_3COOH, AR), oxalic acid dihydrate ($H_2C_2O_4{\cdot}2H_2O$, AR), and calcium chloride ($CaCl_2$, AR) were obtained from Sinopharm Chemical Reagent Company (Shanghai, China). All reagents were of analytical-grade and had no purification. Deionized Millipore-Q water (18.2 MΩ cm) was used during the whole experimentation.

2.2 Sample Preparation

The TiO_2 nanoparticles were synthesized through the sol–gel method. TBT was used as the inorganic precursor, and ethanol and water were used as solvents. First, TBT and ethanol were mixed at a TBT/ethanol volume ratio of 1/2. Meanwhile, a small amount of acetic acid was added under the condition of intense agitation to prevent TBT from reacting with water in the air during the stirring process. Then the deionized water was dropped into the TBT solution with vigorous stirring. In the preparation, the volume ratio of H_2O, TBT, and ethanol is kept at 7:17:34. The ER fluid was stirred for 12 h and then aged for 10 h to deposit the particles. Then the white precipitate was filtrated and, using water and ethanol, it was washed three times. Finally, the precipitation was transferred to a vacuum drying oven, vacuum dried at 60°C for 12 h, and then vacuum dehydrated at 120°C for 2 h. The bulk density of the as-prepared TiO_2 particles was 2.0 g/cm^3. The fabrication processing schematic diagram is presented in **Figure 1**.

The calcium–titanium–oxygen precipitate (Ca-Ti-O) nanoparticles were prepared by the co-precipitation method and no special additives were added to the particles (Lu et al., 2007). In brief, calcium chloride, TBT, and absolute ethyl alcohol were the initial solution, and oxalic acid solution was the precipitant. White precipitate came into being as soon as oxalic acid solution was added. After 8 h of aging at room temperature, the precipitation was filtrated and washed. The drying steps were the same as those of TiO_2 nanoparticles. The bulk density of the as-prepared Ca-Ti-O particles was 1.8 g/cm^3.

The ER fluids were obtained by blending the prepared TiO_2 and Ca-Ti-O nanoparticles with silicone oils (50 mPa s at 25°C) via ball milling. The blended ER fluid was dried at 60°C for 1 h before use. The solid content of the ER fluids is denoted by the mass of the ER nanoparticles, e.g., 0.5 g of the TiO_2 nanoparticles blended with 1 ml of silicone oil is denoted by 0.5 g/ml.

2.3 Characterization

The microstructures of the samples were acquired by using Hitachi S4800 field scanning electron microscopy (FE-SEM; Hitachi, Japan) and Tecni F20 transmission electron microscopy (TEM; FEI, United States). By virtue of the Nicolet 6700 transform infrared spectrometer record, Fourier transform infrared (FT-IR; Thermo-Fisher, United States) spectra were from 400 to 4,000 cm^{-1} using KBr pellets. All infrared spectra were collected 32 times the scan data accumulation at a resolution of 4 cm^{-1}. X-ray diffraction (XRD; Bruker, Germany) spectra were obtained by a D8 Advance/Discover diffractometer using Cu kα radiation. Dielectric properties of the powders and ER fluids were performed *via* a broadband dielectric/impedance spectrometer with an Alpha-A analyzer (Novocontrol, Germany). The performed voltage is 1.0 V during the dielectric measurements.

The rheological behaviors of the ER fluid were obtained by the Haake RS6000 rotational rheometer with a 15-mm diameter circular plate, and the gap of the height of the parallel plate is 1 mm (Thermo-Fisher, United States). To get the static yield stress, we adopted a stress–strain measurement at a very low shear rate (0.2 rad/s), and the yield stress is the stress value when the viscosity decreases

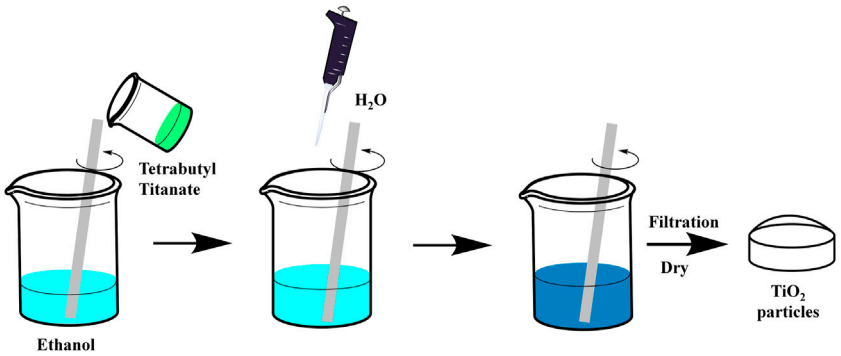

FIGURE 1 | The fabrication processing schematic diagram of TiO_2 particles.

abruptly. The shear stress vs. shear rate curve of the ER was measured using the CR mode with shear rates from 1 to 100 s^{-1}. The external electric field was generated from the SL 300 DC high-voltage generator (Spellman, United States). The controlled humidity environments were achieved by placing in a temperature humidity chamber for calibration at a set humidity for 5 h. Experimental data were carried out with the aid of the software package Rheowin. All data were accomplished at room temperature.

3 RESULTS AND DISCUSSION

3.1 Characterization of the Dielectric Nanoparticles

The size and shape of the TiO_2 particles were examined by SEM and TEM. From **Figure 2A**, it can be observed that the particles have a spherical shape and a rather uniform size distribution, or some irregular agglomerates. The primary particle size is less than 500 nm. The TEM image (inset in **Figure 2A**) reveals that the surface of the TiO_2 particle is rough and has tiny little balls sticking around it. The powder XRD patterns of the TiO_2 particles is shown in **Figure 2B**. The pattern almost is a smooth line without the characteristic peak of a TiO_2 crystal, which indicates the amorphous structure of the TiO_2 particles. **Figure 2C** is the infrared spectra of the TiO_2 particles. The wide peak from 2,900 to 3,500 cm^{-1} is derived from the asymmetric and symmetric stretching vibration of the −OH group. The peak around 1,647 cm^{-1} is assignable to the H-O-H bending vibration. The Ti-O band sorption is found in the broad peaks from 900 to 500 cm^{-1}. The peak from 1,455 to 1,380 cm^{-1} is assignable to CH_2 and CH_3 in-plane deformation distortion, which indicates a small amount of CH_3 and CH_2 groups present on the TiO_2 surface. The peak around 1,038 cm^{-1} is attributed to the C-O stretching vibration of butanol. All these data show that the titanium oxide has some residual butanol. These are typical precipitated TiO_2 particles. The dipoles of C=O and O-H are 2.3~2.7 and 1.51 Debye, respectively. Based on the mechanism of the giant ER effect proposed, sufficient active groups on the surfaces of the particles would promote ER response (Shen et al., 2009).

3.2 Electrorheological Properties of Electrorheological Fluids

The particle distribution of the TiO_2 ER fluids (1.0 g/ml) was observed by an optical microscope (**Figure 3**). Without the electric field, the TiO_2 particles are randomly dispersed in the silicone oil. When the electric field strength reaches 0.5 kV/mm, these TiO_2 particles are polarized, and then swiftly form a thick chain-like structure along the direction of the electric field between the positive and negative electrodes. The fibril phenomenon of the TiO_2 particles at the low electric field indicates that the TiO_2 fluids might have high yield stress at the low electric field.

The rheological properties of the TiO_2 ER fluid were evaluated under different electric field strengths. With increasing intensity of electric field strength, the yield stress of the TiO_2 ER fluid significantly rises by several orders of magnitude. When the electric field strength is 2 kV/mm, the yield stress reaches 120 kPa. As the electric field strength increases further, the yield stress deviated from the linearity. Ca-Ti-O is a kind of high-performance electrorheological material (Wang et al., 2005; Cheng et al., 2010; Wu et al., 2016). To compare with our TiO_2 material, we refer to the literature to synthesize Ca-Ti-O electrorheological fluid (The XRD pattern and IR spectrum of Ca-Ti-O particles are shown in **Supplementary Figures S1 and S2**). The yield stress of the Ca-Ti-O ER fluid is only 14.4 kPa at 2.0 kV/mm, which is 15% that of the TiO_2 ER fluid under the same conditions (**Figure 4A** and **Supplementary Figure S3**). Moreover, we noted that the TiO_2 ER fluid demonstrates a much higher ER efficiency [defined as $(\tau_E-\tau_0)/\tau_0$, where τ_E is the shear stress with an electric field, and τ_0 is the shear stress at zero field] than that of Ca-Ti-O ER fluid at the lower applied electric field. The yield stress of TiO_2 ER fluid reached 122.4 kPa at an electric field of 2.0 kV/mm, and the ER efficiency is about 204. The current density is only 8 $\mu A/cm^2$ leaking through the fluids (the relative curves are shown in **Supplementary Figures S4, S6**). In contrast, the yield stress of Ca-Ti-O ER fluid is only 14.4 kPa with an ER efficiency of 6 at 2.0 kV/mm (**Supplementary Figure S5**), which is consistent with the previous report of Shen et al. (2009).

Figure 5 shows the yield stress of TiO_2 ER fluids with different solid particle fractions. It was discovered that the yield stress is

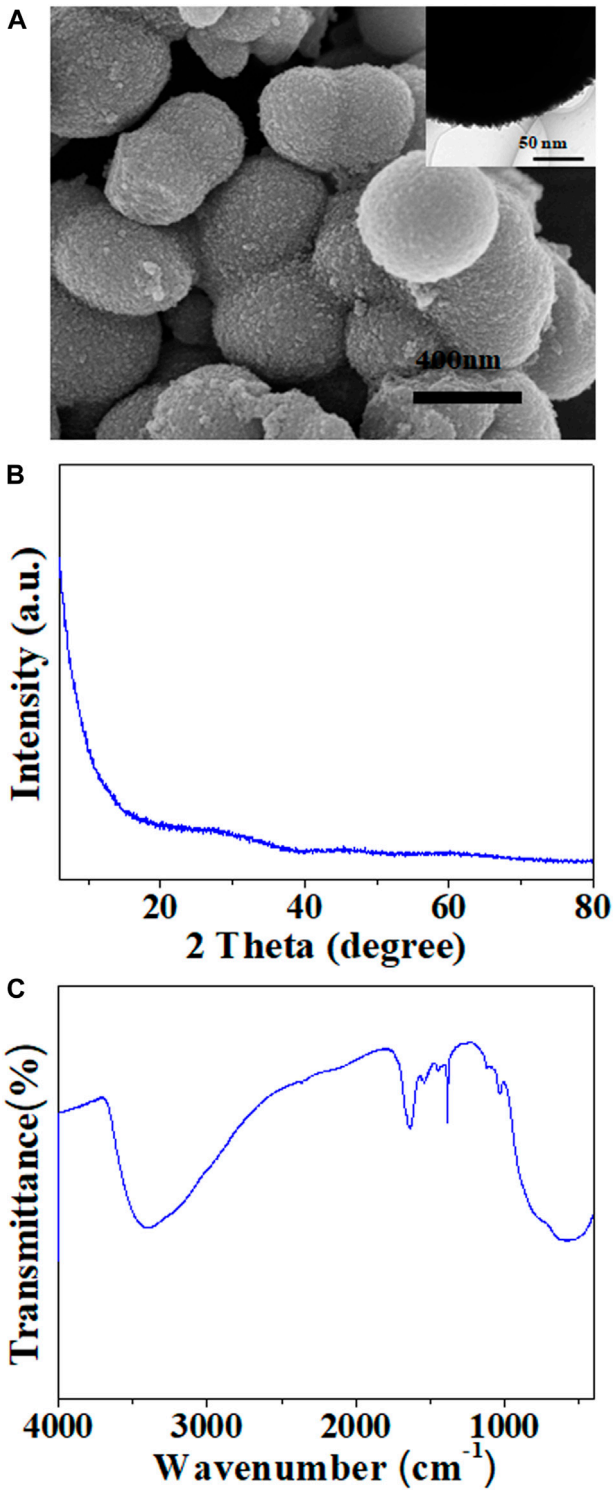

FIGURE 2 | Scanning electron microscopy (SEM) images of **(A)** TiO_2, **(B)** X-ray diffraction (XRD) patterns, and **(C)** the infrared spectra of the TiO_2 particles.

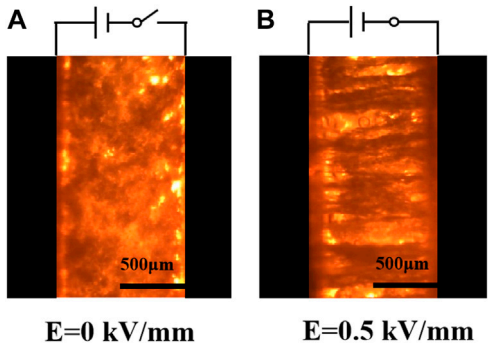

FIGURE 3 | Optical picture of an electrorheological fluid **(A)** without electric field and **(B)** at 0.5 kV/mm.

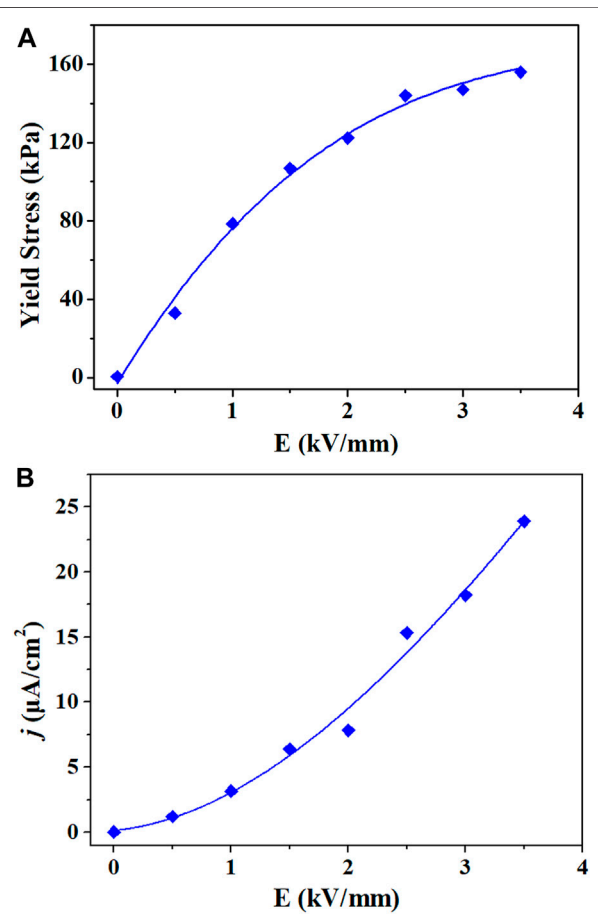

FIGURE 4 | (A) Static yield stress and **(B)** current densities (j) of the prepared electrorheological (ER) fluids at different DC electric fields (solid–liquid ratio of 2 g/ml).

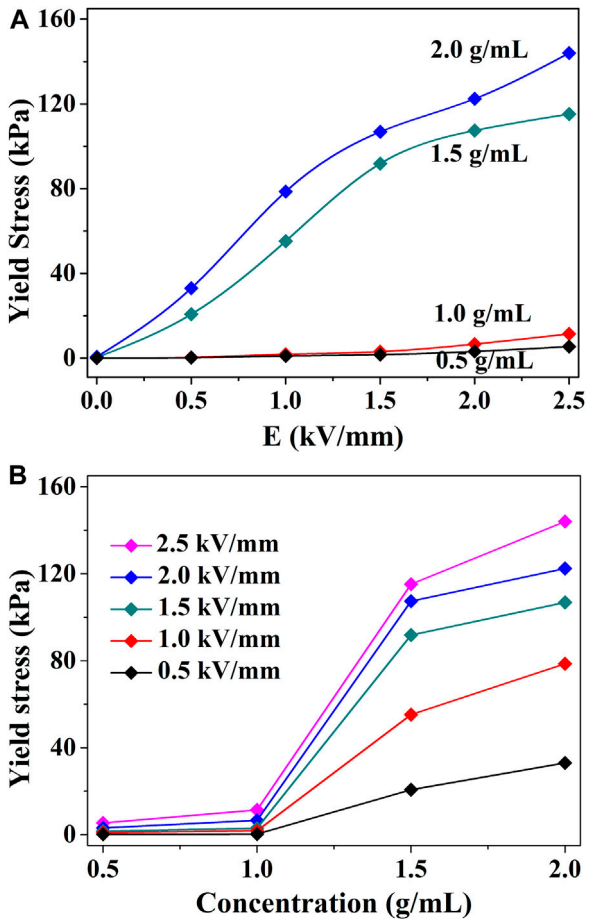

FIGURE 5 | (A) Static yield stress versus electric field strength at different TiO_2 concentrations. **(B)** Static yield stress versus concentration at different electric field strengths.

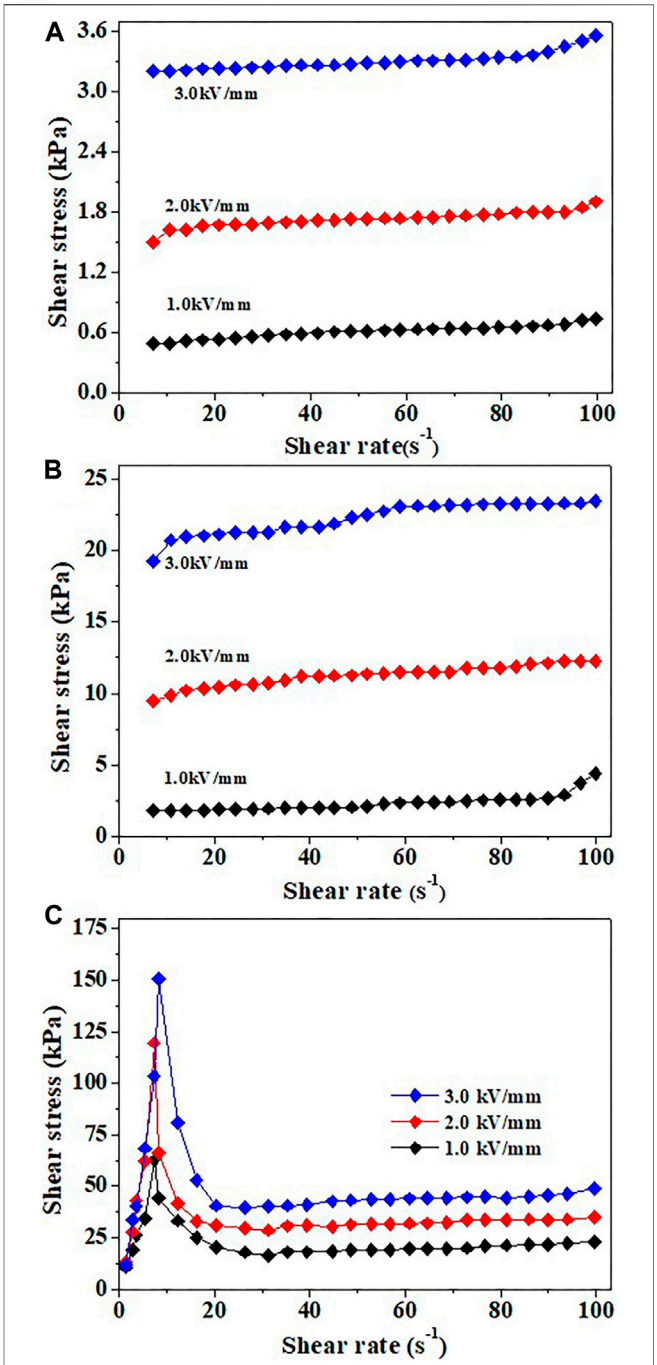

FIGURE 6 | Shear stress as a function of shear rate for **(A)** 0.5, **(B)** 1.0, and **(C)** 2.0 g/ml TiO_2 ER fluids in silicone oil under DC electric field.

positively correlated with the solid concentrations. The yield stress is enhanced with the concentration increasing. When the concentration is less than 1.0 g/ml, the yield stress is small, and the change is not obvious. The yield stress increased significantly from 1.0 to 1.5 g/ml, and the yield stress increased slowly from 1.5 to 2.0 g/ml. When the solid content increases from 1.0 to 1.5 g/ml, the yield stress appears remarkably improved. The yield stress is related to the concentrations of the TiO_2 closely. As for the GER fluids, the high yield stress major comes from the interfacial polarization. Polarized particles will generate interaction force, when the concentration is higher, the distance will be closer. Hence, the interaction force becomes stronger with the concentration. As the solid content further increases, the yield stress is saturated gradually. It is attributed to the polarization (P) of the particles slowed down at high field strengths for high nanoparticle concentrations.

The electric field dependencies of the measured shear stress and solid particle concentrations are shown in **Figure 6**. The shear stress was measured as a function of the shear rate under various electric field strengths (0–3 kV/mm). The ER fluid with low solid content (0.5 and 1.0 g/ml) is a Newtonian fluid when the electric field is zero, and the diagram of shear stress and the shear rate was a constant slash (**Supplementary Figure S7**). After applying the electric field (the ER fluid behaved as a Bingham fluid under an electric field), the dynamic shear stress can reach 3.3 kPa (0.5 g/ml) and 23.5 kPa (1.0 g/ml) at 3 kV/mm, respectively. When the shear rate is added to nearly 100 s^{-1}, the shear stress of the two ER fluids is maintained almost constant (plateau region), which suggested that the process of forming the

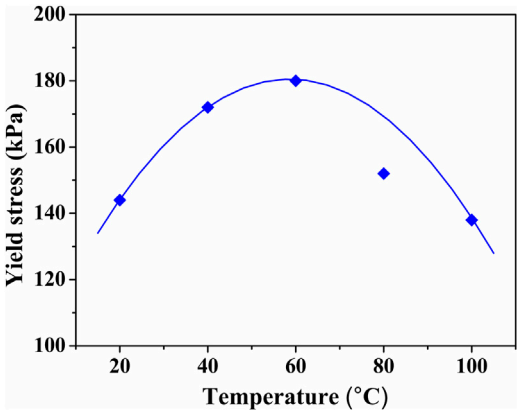

FIGURE 7 | Temperature dependence of the yield stress at E = 2.5 kV/mm of the TiO_2 ER fluid with 2.0 g/ml in silicone oil.

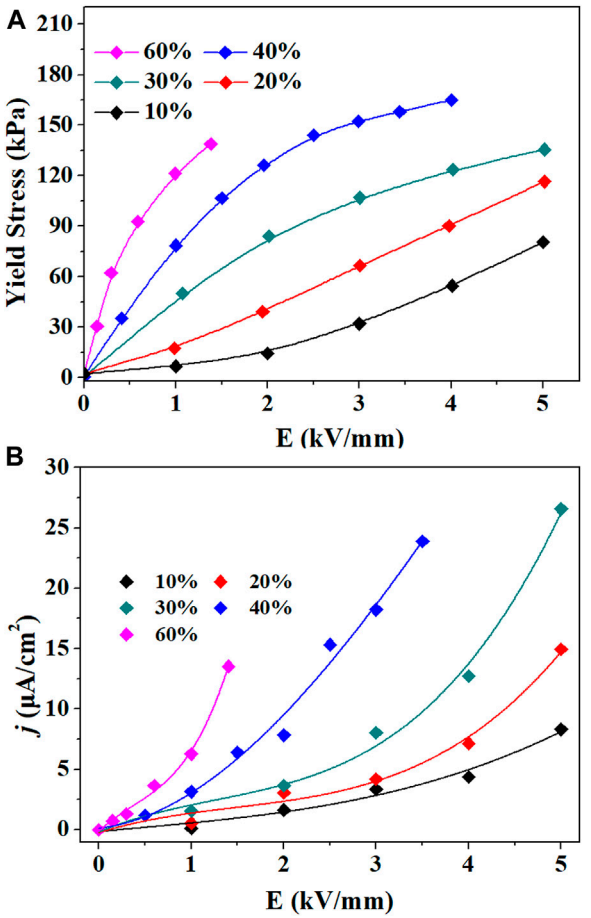

FIGURE 8 | The effect of moisture level on the yield stress **(A)** and corresponding current densities **(B)** of TiO_2 ER fluids with 2.0 g/ml in silicone oil.

chain structure is still dominated by the electrostatic force at low ER fluids. However, when the solid–liquid ratio increased to 2.0 g/ml, the expelling of the ER fluid materials from the center region of the testing apparatus was observed in the concentration and electric field strength applied. Indeed, the expelling behavior is a generic problem encountered in all the parallel plate types of ER measurement apparatus when a higher concentration of ER fluid was used (Gamota and Filisko, 1991). Interestingly, it has been found that the yield stress results from the potential energy of the repulsion between particle chains in an ER fluid (Song et al., 2012). As for the ER fluids shown in **Figure 6C**, when the shear rate was increased to 8~12 s^{-1}, the shear stress has a net reduction due to expelling behavior. Another reason for such behavior may be that the nearest particles separate from the electrode induced by the weaker interaction at the fluid–electrode interface since the commercial electrodes were not made rough (Wang et al., 2007b).

The TiO_2 ER fluids maintain high yield stress during the wide temperature scope from 20°C to 100°C. For representation, the yield stress as a function of temperature for the ER fluid with 2.0 g/ml under various electric field strengths is shown in **Figure 7**. The best yield stress is around 60°C, which is consistent with the permittivity of the TiO_2 particles prepared in a similar way. Taking in the negligible variation of ε in the tested temperature range, the mismatch in ε between TiO_2 and silicone oil would reach a maximum value and leads to a maximum yield stress at around 60°C. Thus, the TiO_2 fluids presented here are preceded by other known ER fluids and have potential applications in fabricating novel ER devices, for instance, clutches and shock absorbers.

3.3 Effect of Water on the Electrorheological Behaviors

For typical inorganic electrorheological materials, the yield stress, apparent viscosity, and leaking current density of the ER fluids passed through its maximum with the moisture content increasing (Espin and Płocharski, 2007), while the yield stress of organic and polymer ER fluids increases monotonously with water content (Wen et al., 1997; Zhang et al., 2001). For typical dielectric-type ER fluids, yield stress data are properly formulated by the power law: $\tau_y \propto E_0^m$ ($m < 2$), where E_0 is the applied electric field (Choi et al., 2001). As indicated in **Figure 8A** and **Supplementary Figure S8**, the yield stress of TiO_2 and Ca–Ti–O ER fluids increases with the water content, and the leaking current increases with the water content as shown in **Figure 8B**, which conforms to the widely accepted dramatic effect of water on the ER effect. However, different trends of yield stress by increasing the electric field strength were observed for ER fluids with different water contents. For TiO_2 ER fluids with very low water content, the slope of E_0 vs. τ_y is $m \approx 2.0$, while the slope approaches 1.0 by increasing the water content. It also showed that there exists a critical value, which corresponds to the giant ER behavior where $m = 1$ at a high electric field. Unexpectedly, a saturation trend is observed over a range of unscaled water contents greater than the critical value, which also resembles the phenomenon in the log–log scale, the slope of 1 at low electric field and becomes 0.4 at high electric field, the reason is that the interficial polarization dominates at low electric field

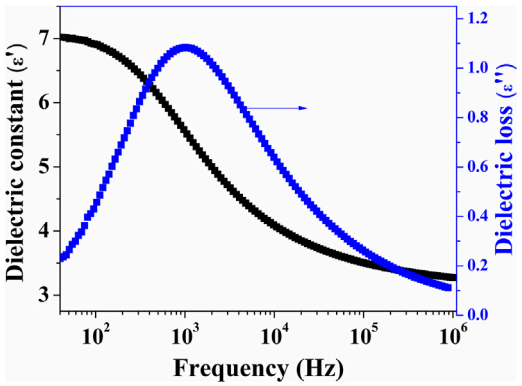

FIGURE 9 | Relaxation spectrum of TiO_2 ER fluids with 2.0 g/ml of silicone oil.

and approach saturation with electric field increasing resulting in the diminishing of the slope (**Supplementary Figure S9**).

So, the action mechanism of moisture in the giant electrorheological fluids is governed by its content. It is easy to form a hydrogen bond bridge between particles in fluids with higher moisture levels with the co-action of the electric field and, hence, the stronger the ER properties. When the moisture content is higher, the "current channel" along the fiber structure of the ER fluid will be formed through the free water in the ER fluids immigrating to the surface of the particles, which screened the dipole–dipole interaction and, hence, the saturation of induced the dipole. The increase in electric field will mainly assist the establishment of the current channel, which reduces the local electric field and increases the yield stress. As for those ER fluids with very low water content, no free water was present, and the absorbed water acts as surface polar molecules, and hence, dielectric-type ER behavior will be observed. Meanwhile, the effect of the temperature and humidity on the yield stress of the TiO_2 ER fluids is researched. The effect is similar for temperature and humidity; both have good yield stress during a wide temperature or humidity range, and the yield stress increases with the humidity at the same temperature and electric field. Compared with the curve of the temperature, they have the same tendency; the yield stress increases and then decreases when the temperature increases (**Supplementary Figure S10**).

3.4 Dielectric Properties of Electrorheological Fluids

It is known that the large polarizability and appropriate dielectric relaxation time of ER particles are critical in producing better and more rapid electrostatic interactions, wherein they can remain as stable structures and rheological properties under shear flow *conditions. Polarizations can be divided into four* contributions: electronic, atomic, Debye (related to the orientation of dipoles), and interfacial polarization (the Maxwell–Wagner polarization). Among them, electronic and atomic polarization are fast polarizations located in the high-frequency range, which could not supply optimal dielectric or polarization properties for high ER activity (Zhao and Yin, 2002a), while Debye and interfacial polarization are appear at the low-frequency range, and their response speeds are slower. It has long been found that in the heterogeneous systems with a clear interface, the strong polarization effect is originated from ion accumulation in the interfacial area, rather than the dipole polarization for the most part. The interfacial polarization, which was properly described by the Wagner model (Wagner, 1914), rather than other polarization including electronic polarization, atomic polarization, and dipole polarization, is generally admitted as that which reflects the underlying physics. When an electric field is applied, two dominant processes occur in the ER fluid simultaneously: one is the polarization of molecules, and the other is the interfacial polarization between clusters.

Figure 9 shows the relaxation spectrum of the as-prepared TiO_2 ER fluids. It can be observed that the permittivity (ε') first decreases and approaches a constant value as the frequency increases. The value of ε' of TiO_2 ER fluid is about six orders smaller than that of Ca-Ti-O ER fluid (**Supplementary Figure S11**), and an obvious dielectric relaxation peak is observed in the TiO_2 ER fluid, while this peak is not found in Ca-Ti-O ER fluid. This may be attributed to its high conductivity; conductivity plays an important role only in the low-frequency range. Through the measurement of the current density, shown in **Figure 4B** and **Supplementary Figure S6**, it is found that both Ca–Ti–O and TiO_2 fluids exhibit the Poole–Frenkel conduction, i.e., $\ln j \propto E^{1/2}$, one of the important features of giant ER fluids (i.e., polar molecule-dominated ER fluids). The current density is obtained by Ohm's law:

$$J = \sigma E \tag{1}$$

where σ is the electrical conductivity. The current density can be written as the product of the mean charge drift velocity v_c and the volume charge density, i.e,

$$J = \rho v_c \tag{2}$$

and substituting this into **Eq. 1**, we have,

$$\sigma = \rho|v_c|/|E| = \rho\mu = (nq)\mu \tag{3}$$

where q is the charge carriers, μ is the mobility of the charge in the electric field, and n is the number density of the charge.

The density of carriers, n, is the fastest varying parameter in this case. Therefore, the electric field-dependent part of the carrier density can be expressed as:

$$n = n_0 \exp(-\Delta V/k_B T) \tag{4}$$

where n_0 is the carrier density in the absent electric field, ΔV is the electrical potential energy of the carrier, k_B is the Boltzmann factor, and T denotes the temperature. Here,

$$\Delta V = q^2/kx + qEx \tag{5}$$

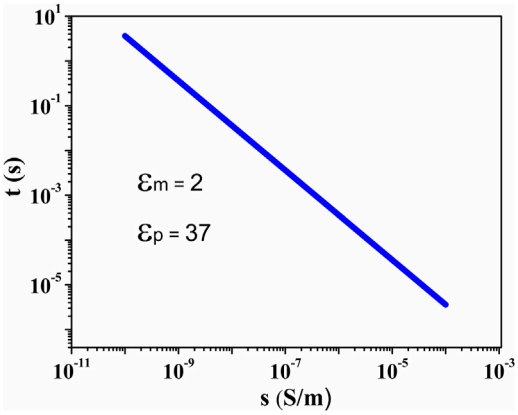

FIGURE 10 | The relaxation time of the interfacial polarization, defined by **Eq. 1**, as a function of particle conductivity. The dielectric constants of silicone oil and TiO_2 particles are 2 and 37, respectively.

where x is the relative distance between the carrier and the electrode. The minimum value of ΔV is at $d\Delta V/dx = 0$. The extremum results can be given by:

$$\left.\frac{d\Delta V}{dx}\right|_{x_0=0} \tag{6}$$

Assuming $\Delta V = -2q^{3/2}\sqrt{E/k}$, for this equation, then we can obtain hbb:

$$\Delta V = 2q^{3/2}\sqrt{E/K} \tag{7}$$

Therefore,

$$\ln J \propto \ln n \propto \Delta V \propto E^{1/2} \tag{8}$$

This behavior is indeed confirmed experimentally. As shown in **Figure 3A** and **Supplementary Figure S3**, a fine linear relation was obtained for both samples, indicating the dominant effect of polar molecules on the ER effect.

For the TiO_2 samples, a distinct dielectric loss, originating from interfacial polarization, which may have a predominant effect on the ER fluid efficiency, was found at 10^3 Hz. For the interfacial polarization, the relaxation time t of one system, when σ_p (conductivity of the particle) >> σ_m (conductivity of the medium), the relationship between σ_p and σ_m can be described as (Morgan, 1934; Hao et al., 1998):

$$t = \varepsilon_0\left(2\varepsilon_m + \varepsilon_p\right)/\sigma_p \tag{9}$$

where ε_0, ε_m, and ε_p are the dielectric constant of the vacuum, continuous (insulating) phase, and disperse (conducting) phase, respectively; σ_p is the conductivity of the dispersed particles (7.2×10^{-6} and 1.5×10^{-5} S/m for TiO_2 and Ca-Ti-O powders at 1 kHz, respectively). Therefore, by virtue of testing the ER fluid response time, we can assume that the relaxation time of the polarization the ER response time would control the relaxation time of the polarization and then govern the ER effect. If the Wagner polarization determines the ER effect in truth, according to **Eq. 1**, the ER fluid answering time should be equivalent to the Wagner polarization relaxation time (Block and Rattray, 1995), which is shown in **Figure 10**. There is an inverse proportional relation between the relaxation time and the particle conductivity. As shown in **Figure 10**, the TiO_2 suspension has a larger conductivity and, hence, a shorter response time. When the ER fluid has a particle conductivity of around 10^{-7} S/m, the response time should be around 1 ms. This improved polarization may be one factor to induce the enhancement of the ER effect of the titania suspension at a lower electric field. Thus, we assume that both Debye and interfacial polarization affect the ER performance. As for the Ca–Ti–O samples, its large dielectric constant is attributed to the polar molecule-coated nanoparticle, whose effective dielectric constant is dominated by its coating and the existence of the interfaces (Wen et al., 2003; Huang et al., 2006; Wang et al., 2007a; Cheng et al., 2008) This induces a large dipole and, thus, a high ER response at a high electric field. (Wen et al., 2003; Huang et al., 2006; Wang et al., 2007a; Cheng et al., 2008; Cheng et al., 2010), while for TiO_2 suspension, the strong ER effect was mainly induced by interfacial polarization.

4 CONCLUSION

We report a novel TiO_2-based ER fluid showing a pronounced ER effect whose yield stress reaches 78.6, 106.8, and 122.4 kPa for an external electric field of only 1, 1.5, and 2 kV/mm, respectively. Dielectric and infrared studies indicate that interfacial polarization dominates in the TiO_2 ER fluid, while polar molecules induced molecular polarization that dominates in the Ca-Ti-O fluid. When carriers are present, they can travel considerable distances through the medium, but when they are captured or cannot be discharged at the electrode, interfacial polarization occurs. The role of water and other polar compounds absorbed on the surface of particles was assumed to induce dielectric loss. The surface polar molecules on both samples were assumed to play a crucial role for their giant electrorheological effect, while interfacial polarization was assumed to be dominated and induces a large yield stress at a low electric field in the TiO_2 ER fluid.

DATA AVAILABILITY STATEMENT

The original contributions presented in the study are included in the article/**Supplementary Material**. Further inquiries can be directed to the corresponding authors.

AUTHOR CONTRIBUTIONS

YC conceptualized the study, formulated the methodology, and wrote the original draft. ZZ validated the study. HW and JW performed the investigation in the study. ZZ and LH performed data curation. ZZ and AS conducted the formal analysis. AS

gathered the resources for the study. JW and GX supervised the study. ZL validated the study. YC, ZL, and JG reviewed the original draft. JG edited the manuscript. GX was in charge of the project administration.

FUNDING

This research is funded by the National Natural Science Foundation of China (11874366), the Ningbo Natural Science Foundation (2018A610167, 2018A610322), and the Open Project Program of Fujian Key Laboratory of Functional Marine Sensing Materials, Minjiang University (MJUKF-FMSM201908).

SUPPLEMENTARY MATERIAL

The Supplementary Material for this article can be found online at: https://www.frontiersin.org/articles/10.3389/fmats.2021.764455/full#supplementary-material

REFERENCES

Almajdalawi, S., Pavlinek, V., Mrlik, M., Cheng, Q., and Sedlacik, M. (2013). Synthesis and Electrorheological Effect of Cr Doped TiO_2 nanorods with Nanocavities in Silicone Oil Suspensions. *J. Phys. Conf. Ser.* 412, 012003. doi:10.1088/1742-6596/412/1/012003

Block, H., and Rattray, P. (1995). Recent Developments in ER Fluids. *Prog. Electrorheology*, 19–42. doi:10.1007/978-1-4899-1036-3_3

Cheng, Y., Guo, J., Xu, G., Cui, P., Liu, X., Liu, F., et al. (2008). Electrorheological Property and Microstructure of Acetamide-Modified TiO2 Nanoparticles. *Colloid Polym. Sci.* 286, 1493–1497. doi:10.1007/s00396-008-1920-0

Cheng, Y., Wu, K., Liu, F., Guo, J., Liu, X., Xu, G., et al. (2010). Facile Approach to Large-Scale Synthesis of 1D Calcium and Titanium Precipitate (CTP) with High Electrorheological Activity. *ACS Appl. Mater. Inter.* 2, 621–625. doi:10.1021/am900841m

Choi, H. J., Cho, M. S., Kim, J. W., Kim, C. A., and Jhon, M. S. (2001). A Yield Stress Scaling Function for Electrorheological Fluids. *Appl. Phys. Lett.* 78, 3806–3808. doi:10.1063/1.1379058

Espin, M. J., and Płocharski, J. (2007). Effect of Pollution on the Interfacial Properties of Electrorheological Fluids. *Colloids Surf. A: Physicochemical Eng. Aspects* 306, 126–136. doi:10.1016/j.colsurfa.2006.10.033

Gamota, D. R., and Filisko, F. E. (1991). Dynamic Mechanical Studies of Electrorheological Materials: Moderate Frequencies. *J. Rheology* 35, 399–425. doi:10.1122/1.550221

Halsey, T. C. (1992). Electrorheological Fluids. *Science* 258, 761–766. doi:10.1126/science.258.5083.761

Hao, T., Kawai, A., and Ikazaki, F. (1998). Mechanism of the Electrorheological Effect: Evidence from the Conductive, Dielectric, and Surface Characteristics of Water-free Electrorheological Fluids. *Langmuir* 14, 1256–1262. doi:10.1021/la971062e

He, K., Wen, Q., Wang, C., Wang, B., Yu, S., Hao, C., et al. (2018). A Facile Synthesis of Hierarchical Flower-like TiO2 Wrapped with MoS2 Sheets Nanostructure for Enhanced Electrorheological Activity. *Chem. Eng. J.* 349, 416–427. doi:10.1016/j.cej.2018.05.102

He, K., Wen, Q., Wang, C., Wang, B., Yu, S., Hao, C., et al. (2017). The Preparation and Electrorheological Behavior of Bowl-like Titanium Oxide Nanoparticles. *Soft Matter* 13, 7677–7688. doi:10.1039/c7sm01157a

Huang, X., Wen, W., Yang, S., Sheng, P., and Sheng, P. (2006). Mechanisms of the Giant Electrorheological Effect. *Solid State. Commun.* 139, 581–588. doi:10.1016/j.ssc.2006.04.042

Hwang, Y.-H., Kang, S.-R., Cha, S.-W., and Choi, S.-B. (2016). An Electrorheological Spherical Joint Actuator for a Haptic Master with Application to Robot-Assisted Cutting Surgery. *Sensors Actuators A: Phys.* 249, 163–171. doi:10.1016/j.sna.2016.08.033

Ji, X., Zhang, W., Jia, W., Wang, X., Tian, Y., Deng, L., et al. (2017). Cactus-like Double-Shell Structured SiO 2 @TiO 2 Microspheres: Fabrication, Electrorheological Performances and Microwave Absorption. *J. Ind. Eng. Chem.* 56, 203–211. doi:10.1016/j.jiec.2017.07.013

Kim, M. H., Bae, D. H., Choi, H. J., and Seo, Y. (2017). Synthesis of Semiconducting Poly(diphenylamine) Particles and Analysis of Their Electrorheological Properties. *Polymer* 119, 40–49. doi:10.1016/j.polymer.2017.05.017

Lu, K., Shen, R., Wang, X., Sun, G., Wen, W., and Liu, J. (2007). Polar Molecule Type Electrorheological Fluids. *Int. J. Mod. Phys. B* 21, 4798–4805. doi:10.1142/s0217979207045682

Morgan, S. O. (1934). Two Types of Dielectric Polarization. *Trans. Electrochem. Soc.* 65, 109–118. doi:10.1149/1.3498002

Niu, C., Dong, X., Zhao, H., and Qi, M. (2014). Properties of Aniline-Modified Strontium Titanyl Oxalate-Based Electrorheological Suspension. *Smart Mater. Struct.* 23, 075018. doi:10.1088/0964-1726/23/7/075018

Plachy, T., Mrlik, M., Kozakova, Z., Suly, P., Sedlacik, M., Pavlinek, V., et al. (2015). The Electrorheological Behavior of Suspensions Based on Molten-Salt Synthesized Lithium Titanate Nanoparticles and Their Core-Shell Titanate/Urea Analogues. *ACS Appl. Mater. Inter.* 7, 3725–3731. doi:10.1021/am508471f

Shen, R., Wang, X., Lu, Y., Wang, D., Sun, G., Cao, Z., et al. (2009). Polar-Molecule-Dominated Electrorheological Fluids Featuring High Yield Stresses. *Adv. Mater.* 21, 4631–4635. doi:10.1002/adma.200901062

Shen, R., Wang, X., Wen, W., and Lu, K. (2005). Tio2Based Electrorheological Fluid with High Yield Stress. *Int. J. Mod. Phys. B* 19, 1104–1109. doi:10.1142/s0217979205029924

Song, Z., Cheng, Y., Wu, J., Guo, J., and Xu, G. (2012). Influence of Volume Fraction on the Yield Behavior of Giant Electrorheological Fluid. *Appl. Phys. Lett.* 101, 101908. doi:10.1063/1.4751264

Su, J., Cheng, H., Wen, Y., Feng, Y., and Tam, H.-Y. (2016). Investigation into the Mechanism for Ultra Smooth Electrorheological Finishing Using Wheel-like Finishing Tool. *J. Mater. Process. Technology* 238, 124–131. doi:10.1016/j.jmatprotec.2016.07.019

Tao, R., Tang, H., Tawhid-Al-Islam, K., Du, E., and Kim, J. (2016). Electrorheology Leads to Healthier and Tastier Chocolate. *Proc. Natl. Acad. Sci. USA* 113, 7399–7402. doi:10.1073/pnas.1605416113

Wagner, K. W. (1914). Erklärung der dielektrischen Nachwirkungsvorgänge auf Grund Maxwellscher Vorstellungen. *Archiv F. Elektrotechnik* 2, 371–387. doi:10.1007/bf01657322

Wang, B.-X., Zhao, X.-P., Zhao, Y., and Ding, C.-L. (2007). Titanium Oxide Nanoparticle Modified with Chromium Ion and its Giant Electrorheological Activity. *Composites Sci. Technology* 67, 3031–3038. doi:10.1016/j.compscitech.2007.05.004

Wang, B.-X., Zhao, Y., and Zhao, X.-P. (2007). The Wettability, Size Effect and Electrorheological Activity of Modified Titanium Oxide Nanoparticles. *Colloids Surf. A: Physicochemical Eng. Aspects* 295, 27–33. doi:10.1016/j.colsurfa.2006.08.025

Wang, B., and Zhao, X. (2003). Preparation of Kaolinite/titania Coated Nanocomposite Particles and Their Electrorheological Properties. *J. Mater. Chem.* 13, 2248–2253. doi:10.1039/b305718f

Wang, X., Shen, R., Wen, W., and Lu, K. (2005). High Performance Calcium Titanate Nanoparticle ER Fluids. *Int. J. Mod. Phys. B* 19, 1110–1113. doi:10.1142/s0217979205029936

Wen, W., Huang, X., and Sheng, P. (2008). Electrorheological Fluids: Structures and Mechanisms. *Soft Matter* 4, 200–210. doi:10.1039/b710948m

Wen, W., Huang, X., and Sheng, P. (2004). Particle Size Scaling of the Giant Electrorheological Effect. *Appl. Phys. Lett.* 85, 299–301. doi:10.1063/1.1772859

Wen, W., Huang, X., Yang, S., Lu, K., and Sheng, P. (2003). The Giant Electrorheological Effect in Suspensions of Nanoparticles. *Nat. Mater* 2, 727–730. doi:10.1038/nmat993

Wen, W., Ma, H., Tam, W. Y., and Sheng, P. (1997). Frequency and Water Content Dependencies of Electrorheological Properties. *Phys. Rev. E* 55, R1294–R1297. doi:10.1103/physreve.55.r1294

Whittle, M., and Bullough, W. A. (1992). The Structure of Smart Fluids. *Nature* 358, 373. doi:10.1038/358373a0

Wu, J., Song, Z., Liu, F., Guo, J., Cheng, Y., Ma, S., et al. (2016). Giant Electrorheological Fluids with Ultrahigh Electrorheological Efficiency Based on a Micro/nano Hybrid Calcium Titanyl Oxalate Composite. *NPG Asia Mater.* 8, e322. doi:10.1038/am.2016.158

Yin, J. B., and Zhao, X. P. (2004a). Giant Electrorheological Activity of High Surface Area Mesoporous Cerium-Doped TiO_2 Templated by Block Copolymer. *Chem. Phys. Lett.* 398, 393–399. doi:10.1016/j.cplett.2004.09.098

Yin, J. B., and Zhao, X. P. (2004b). Preparation and Enhanced Electrorheological Activity of TiO_2 Doped with Chromium Ion. *Chem. Mater.* 16, 321–328. doi:10.1021/cm034787e

Zhang, J., Tao, D., and Zhang, Z. (2001). Effect of Moisture on the Electrorheological Properties of Chitosan and Chitosan-Cu^{2+} Complex Polyelectrolyte Particles. *Tribology* 21, 131–134.

Zhao, X. P., and Yin, J. B. (2002). Preparation and Electrorheological Characteristics of Rare-Earth-Doped TiO2 Suspensions. *Chem. Mater.* 14, 2258–2263. doi:10.1021/cm011522w

Zhao, X. P., Zhao, Q., and Gao, X. M. (2003). Optical Activity of Electrorheological Fluids under External Electric Field. *J. Appl. Phys.* 93, 4309–4314. doi:10.1063/1.1559435

Zhao, X., and Yin, J. (2002). Preparation and Electrorheological Activity of Mesoporous Rare-Earth-Doped TiO2. *Chem.Mater.* 14, 4633–4640. doi:10.1021/cm011522w

Conflict of Interest: The authors declare that the research was conducted in the absence of any commercial or financial relationships that could be construed as a potential conflict of interest.

Publisher's Note: All claims expressed in this article are solely those of the authors and do not necessarily represent those of their affiliated organizations, or those of the publisher, the editors, and the reviewers. Any product that may be evaluated in this article, or claim that may be made by its manufacturer, is not guaranteed or endorsed by the publisher.